Toroidal Structure of Hydrogen Recycling in Ultra-long Discharges on TRIAM-1M

M. Sakamoto[1)], Y. Matsuo[2)], H. Zushi[1)], K. Nakamura[1)], K. Hanada[1)], K.N. Sato[1)], H. Idei[1)], M. Hasegawa[1)], A. Iyomasa[1)], S. Kawasaki[1)], H. Nakashima[1)], A. Higashijima[1)], T. Kuramoto[2)], M. Kitaguchi[2)], T. Sugata[2)], N. Maezono[2)], N. Yoshida[3)], K. Tokunaga[3)], T. Fujiwara[3)], M. Miyamoto[3)], M. Tokitani[2)], Y. Nakashima[4)], Y. Kubota[4)], Y. Higashizono[4)], Y. Hirooka[5)], S. Kado[6)], T. Shikama[6)]

1) Advanced Fusion Research Center, Research Institute for Applied Mechanics, Kyushu University, Kasuga, Fukuoka 816-8580, Japan
2) Interdisciplinary Graduate School of Engineering Sciences, Kyushu University, Fukuoka, Japan
3) Research Institute for Applied Mechanics, Kyushu University, Fukuoka, Japan
4) University of Tsukuba, Ibaraki, Japan
5) National Institute for Fusion Science, Gifu, Japan
6) The University of Tokyo, Tokyo, Japan

E-mail: sakamoto@triam.kyushu-u.ac.jp

Abstract. The ultra-long discharge with the duration of 5 h 16 min has been achieved using the ML with good cooling capability in TRIAM-1M. The temperature increase in the plasma facing components could be successfully suppressed by the movable limiter (ML). The wall inventory continued to increase during the discharge and finally reached up to 8 x 10^{21} atoms at the end of the discharge. No Long time global balance between particle absorption and release of the wall was observed. The averaged wall pumping rate is evaluated to be ~8.6 x 10^{16} atoms m^{-2} s^{-1}, which is about 3.6 times higher than that evaluated in the previous ultra-long discharge without the ML. It seems to be attributed to suppression of the hydrogen release from the wall due to less temperature increase. The toroidal structure of hydrogen recycling changes only at the ML and its neighborhood, and the other part, i.e. main chamber recycling, still remain the same structure as that without the ML. Moreover, it is found that the structure of the main chamber recycling is the same in the low and high density cases. It suggests that the charge exchange neutral dominates the main chamber recycling. The contribution ratio of the main chamber to the wall recycling decreases by about half due to the ML. That of the section of the ML reaches about 45%.

1. Introduction

Steady state operation (SSO) is one of the most important issues for the future fusion reactor. As a discharge duration grows longer, phenomena with long characteristic time such as current diffusion and plasma-wall equilibrium times play more important role for the SSO. The particle balance in the main chamber is one of those and it is important from the viewpoint of the density control. The wall plays a role of the particle sink and source. The wall temperature is a key for the particle source and the co-deposition is a key for the particle sink. In Tore Supra, an uncontrolled density increase due to outgassing from uncooled and poorly conditioned in-vessel components had been observed in the high power and long duration discharge, but it has not been observed and continuous wall pumping has been observed after upgrading the plasma facing components (PFCs) [1-3]. Also in TRIAM-1M, the importance of the wall temperature and the co-deposition for the global particle balance has been reported [4-7]. The global particle balance depends on local recycling, which is a strong function of space and time [8-12]. A spatial structure of wall recycling is important for understanding the global particle balance in the SSO.

In the last year, TRIAM-1M established a world record for discharge duration of 5h 16 min using a movable limiter (ML) with good cooling capability [13]. The temperature increase of the plasma facing components can be well suppressed due to the insert of the ML. The impact of the suppression of the temperature increase on the global particle balance and the toroidal structure of the wall recycling with and without the ML will be presented.

2. Experimental Set Up

One of the features of the TRIAM-1M tokamak (R_{major} ~ 0.8 m, $a \times b$ = 0.12 m x 0.18 m) is that all of the plasma facing components are made of high Z materials: the poloidal limiters and the divertor plates are made of molybdenum, and the main chamber is made of stainless steel. A low Z material coating has never been done. The ML of which front edge is made of molybdenum has been installed at the same section as the fixed poloidal limiter (PL) and the pumping port. It is thermally insulated from the main chamber and has good cooling capability. As shown in Fig.1, the ML can be approached from above to the plasma by remote control.

The amount of hydrogen injected in the main chamber through the piezoelectric valve is controlled by feedback to match the H_α intensity ($I_{H\alpha}$) at the central chord with the reference signal. Namely, the hydrogen influx is feedback controlled, since $I_{H\alpha}$ is a measure of the number of hydrogen atoms that are ionized per unit time. The H_α signal for the fueling control is measured horizontally at #3 section shown in Fig.2. The hydrogen gas is supplied at #6 section. The neutral gas in the main chamber is evacuated by a turbo-molecular-pump of which effective pump speed is about 0.55 m^3/s.

In order to study the structure of hydrogen recycling, a toroidal profile of $I_{H\alpha}$ has been measured at 7 sections in the toroidal direction as shown in Fig.2. Poloidal profiles have also been measured at each section except #4 section. The direction of the line of sight of H_α measurement is vertical except #4 section of which direction is horizontal. The ML is located at #1 section. It is noted that all results reported in this paper were obtained in hydrogen discharges with a limiter configuration.

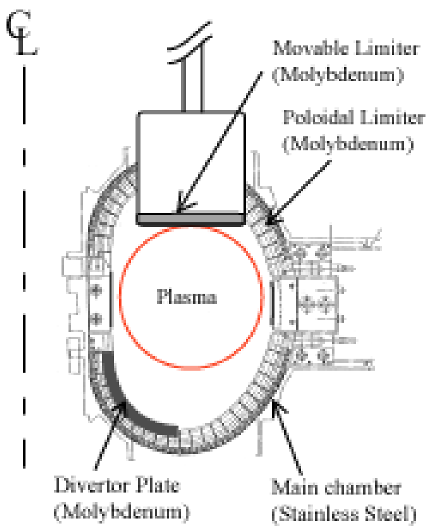

Fig.1 Cross-sectional view of the main chamber at the section of the movable limiter.

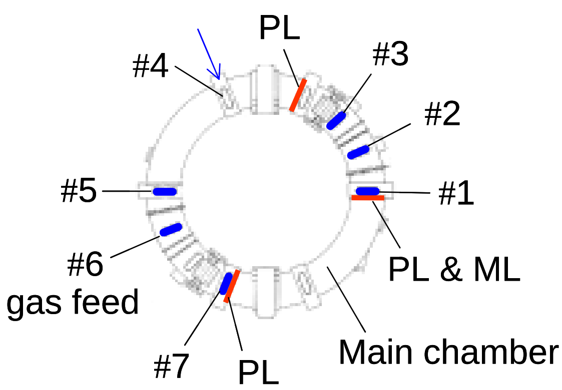

Fig.2 Top view of the main chamber. Three sets of the poloidal limiters (PL) are installed. The movable limiter (ML) is installed at #1 section. The hydrogen gas is injected from below of the torus at #6 section. The H_α intensity measured at #1-#7 sections.

3. Experimental Results and Discussion

3.1. Impact of the Movable Limiter on the Global Particle Balance

Figure 3 shows the waveforms of 5 h 16 min discharge. The plasma current was sustained by 2.45 GHz LHCD (P_{rf}~6kW) and was almost constant at ~15 kA during the discharge. The injected energy finally reached ~0.11 GJ. The plasma density is deduced to be ~1 x 10^{18} m^{-3}. The gas fueling was feedback controlled to keep $I_{H\alpha}$, i.e. hydrogen influx to the plasma, constant as shown in Fig.3 (b). In this discharge, the ML is used to reduce the heat load to the other PFCs. The increase in the temperature of the main chamber and the PL could be successfully suppressed by ~30% and ~70% of those of the ultra-long discharge without the ML, respectively. The heat loads to each PFC of the discharge with and without the ML are the following; the main chamber 56% and 70%, the fixed limiters 10% and 30%, the movable limiter 34% and 0%, which are estimated using the calorimetry. The temperature near the bellows of the main chamber, of which temperature had increased up to 120 ^{o}C in the previous ultra-long discharge without the ML [7], increased only less than 60 ^{o}C as shown in Fig.3 (c). The increase in impurity influx was not observed during the whole discharge time as shown in Fig.3 (d) and (e), although many spikes were observed in MoI intensity. Those spikes seem to be caused by small dusts.

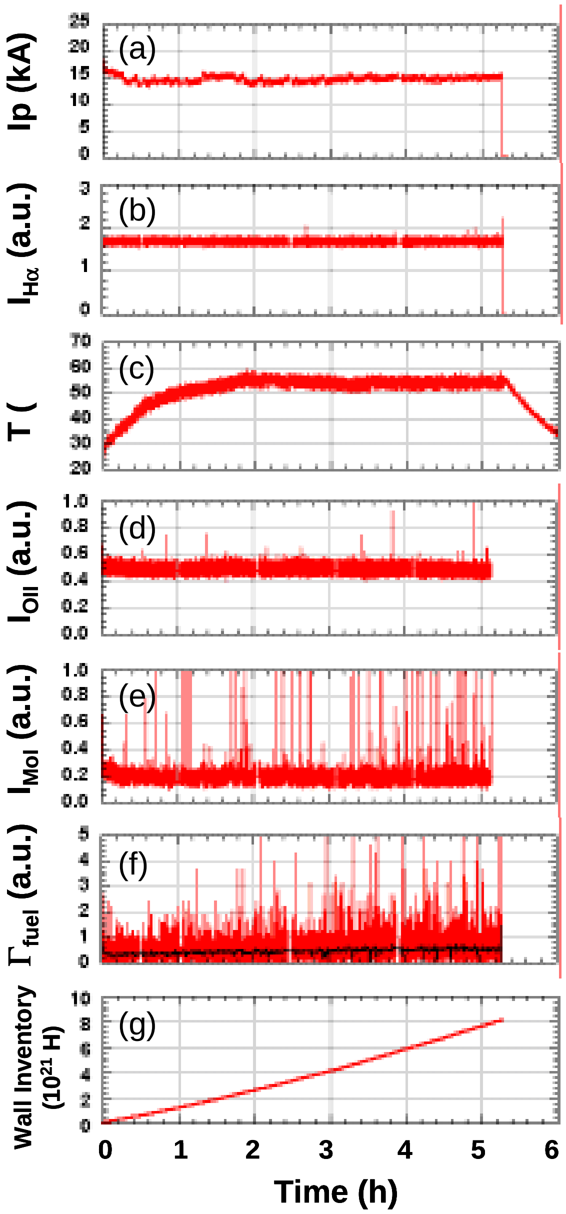

Fig. 3 Time evolution of (a) plasma current, (b) H_{α} intensity, (c) wall (bellows) temperature, which is measured by the thermo couple, (d) OII intensity, (e) MoI intensity, (f) fueling rate and (g) wall inventory in the long duration discharge with the duration of 5 h 16 min.

In the latter phase of the discharge, the piezo-electric valve was automatically closed so as to keep $I_{H\alpha}$ but the duration of no fueling was only a few tens seconds. Long time global balance between particle absorption and release of the wall was not observed. As shown in Fig.3 (f), the fueling rate Γ_{fuel} gradually increased during the discharge and it reached about 5.5 x 10^{17} atoms s^{-1}. It should be noted that four gaps in the data of Fig.3 (f) are attributed to the data storage from the memory of ADC and those do not mean the wall saturation. The wall inventory can be evaluated using a particle balance between fueling and pumping rates and it reaches up to 8 x 10^{21} atoms as shown in Fig.3 (g). The global wall pumping rate is estimated to be ~4.3 x 10^{17} atoms s^{-1}. If an area of particle loading is the whole surface

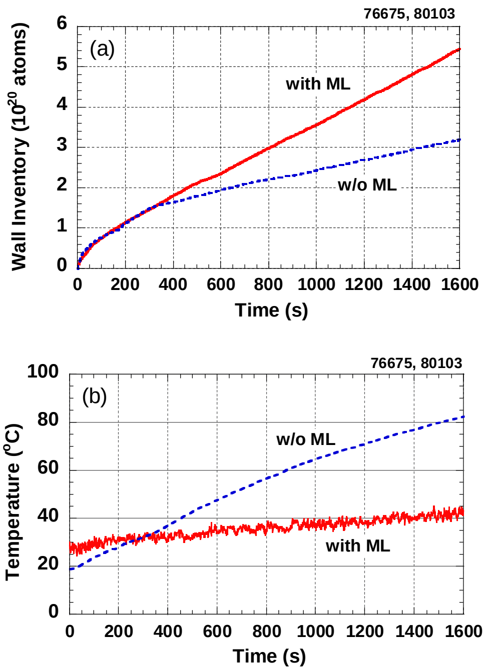

Fig.4 Time evolution of (a) wall inventory and (b) wall (bellows) temperature of the long duration discharges with and without the ML.

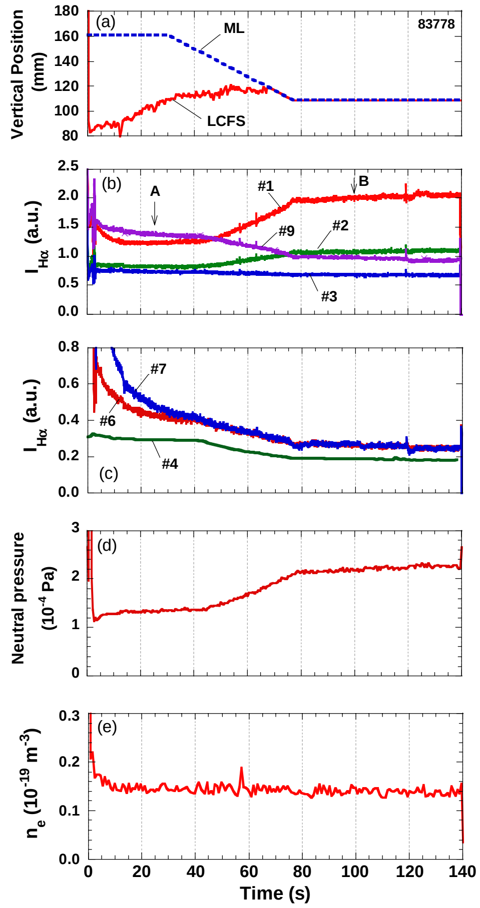

Fig. 5 Time evolution of (a) position of the ML and the LCFS, (b) H_α intensity at #1,2,3,9 sections, (c) H_α intensity at #4,6,7 sections, (d) neutral pressure at the pump duct and (e) line averaged electron density.

area (~5m^2) of the main chamber, the wall pumping rate is ~8.6 x 10^{16} atoms m^{-2} s^{-1}. This value is about 3.6 times higher than that evaluated in the previous ultra-long discharge without the ML [7]. Because the net wall pumping rate means the balance between the hydrogen absorption rate and hydrogen release rate of the wall. The difference in the wall pumping rates between the present discharge and the previous one, i.e. with and without ML, suggests that the hydrogen release from the wall is suppressed due to less temperature increase by the insert of the ML. Actually, the time trace of the wall inventories after the discharge initiation of both discharges is the almost same until ~330 s and afterwards the difference between the wall inventories widens as the temperature of the main chamber of the discharge without the ML increases as shown in Fig. 4.

3.2. Structure of the Wall Recycling

As seen in the above section, the movable limiter gives a great impact on the global particle balance. So, we have investigated the spatial structure of the wall recycling with and without the ML. In this experiment, the ML was initially set sufficiently away from the last closed flux surface (LCFS) and it was inserted to the LCFS from t~30 s as shown in Fig.5 (a). The position of the LCFS is estimated assuming that the plasma cross-section is circular. The ML finally limited the LCFS. The effect of the ML starts to appear when the distance between the ML and the LCFS is about 30 mm. The H_α intensity at #1 (i.e. ML position) and #2 sections increased due to the interaction between the ML and the plasma. That at #3 section kept almost constant. The other signals decreased due to the insert of the ML. The reason of the decrease in $I_{H\alpha}$ is thought to be that the ML disturbs neutral particles' traveling through the SOL and it becomes difficult for neutral hydrogen to go around. On the other hand, the neutral pressure at the pumping duct increased as the same rate of $I_{H\alpha}$ at #1 section. It is reasonable, since the ML is located at the same section as the pumping port and the neutral hydrogen concentrates on the ML. It is noted that the line averaged electron density did not change against the insert of the ML as shown in Fig.5 (e) although $I_{H\alpha}$ at each section dramatically changed.

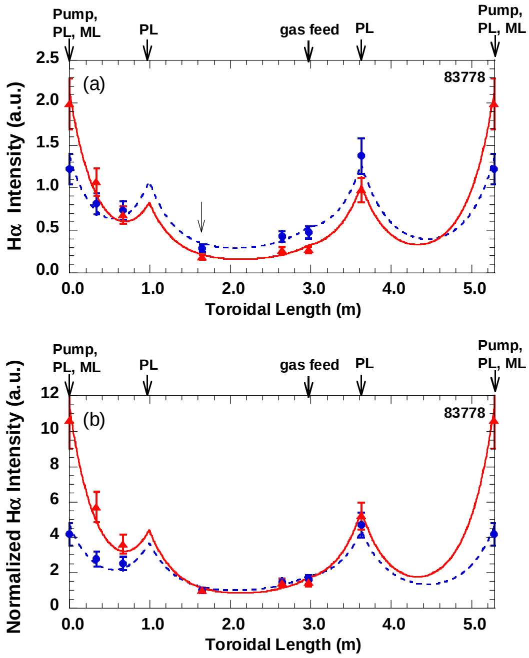

Fig.6 (a) Toroidal profiles of the H_α intensity before (circle, dotted line) and after (triangle, solid line) the insert of the ML and (b) profiles normalized by the data indicated by the arrow in (a).

Figure 6 (a) shows the toroidal profiles of $I_{H\alpha}$ at the central chord before and after the insert of the ML, i.e. at the time indicated by arrows A and B in Fig.5 (b), respectively. The origin of the horizontal axis means the position of the ML (i.e. #1 section) and the toroidal length is the circumferential length along the plasma center. The right end of the figure means a full circle. Fig.6 (b) shows the profiles normalized by the intensity at #4 section, since that intensity has least influence of the limiter and the fueling. The effect of the ML on the recycling structure is localized only near the ML. The part except the ML and its neighborhood still remains the same structure as that without the ML as shown in Fig.6 (b). It means that the structure of the main chamber recycling has less influence of the insert of the ML. It suggests that the charge exchange neutral dominates the main chamber recycling, since they are not concerned with the structure of the magnetic flux surface.

The profile is reproduced according to the following fitting equation;

$$I_{H\alpha}(x) = P_{mc} + \sum_{i=1}^{3} P_i \exp\left[\frac{-|x - x_i|}{\lambda_{LIM}}\right] + P_{gf} \exp\left[\frac{-|x - x_{gf}|}{\lambda_{gf}}\right], \qquad (1)$$

where x is the toroidal length. P_{mc} is contribution of the main chamber recycling and is assumed to be homogeneous in the toroidal direction, since the structure of the main chamber recycling has less influence of the limiter as mentioned above. The second and third terms of the right-hand side mean the contributions of the limiters and gas feed, respectively. As shown in Fig.6 (a), we can reproduce the measured profile when λ_{LIM} is 0.33 m and $\lambda_{gf} = 2\lambda_{LIM}$. The contribution ratio of the main chamber and the limiters including the ML to the hydrogen recycling is the following; 33% and 59% before the insert of the ML, and 18% and 78% after the insert of the ML. The contribution ratio of the section of the ML is ~45%. That of the main chamber decreases by about half due to the insert of the ML. Integration of $I_{H\alpha}$ over the whole toroidal length is about the same within 10%, which is less than the error, i.e. 15%. This seems to be a reason why the density did not change before and after the insert of the ML.

Figure 7 shows a comparison of the toroidal profiles of $I_{H\alpha}$ between low ($\bar{n}_e$~0.1x10^{19} m^{-3}) and high density ($\bar{n}_e$~1x10^{19} m^{-3}) discharges with the ML. Both profiles are normalized by the intensity at #4 section shown in Fig.2. The structure of the main chamber recycling remains the same structure even though the density changes by the one order of magnitude. It suggests again the relation between the charge exchange neutrals and the main chamber recycling. In the high density case, λ_{LIM} is 0.22 m to reproduce the toroidal profile of $I_{H\alpha}$. It is two third of that of the low density case. The mean free path cannot explain the difference of λ_{LIM} between the low and the high density discharges. When the density is 1x10^{19} m^{-3}, the mean free path of the Franck-Condon hydrogen is only about 0.04 m. The broadening of the profile at the limiter may be attributed to the transport of the neutrals through the SOL.

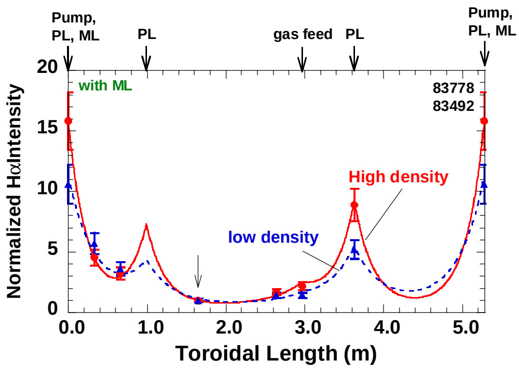

Fig. 7 Normalized profiles of low (0.1 x 10^{19} m^{-3}, triangle, dotted line) and high (1 x 10^{19} m^{-3}, circle, solid line) density discharges with the ML. The normalized point is indicated by the arrow.

4. Summary

In TRIAM-1M, the ultra-long discharge with the duration of 5 h 16 min has been achieved using the ML with good cooling capability. The temperature increase in the PFCs could be successfully suppressed by the ML. From the particle balance between the fueling and pumping rates, the averaged wall pumping rate is evaluated to be ~8.6 x 10^{16} atoms m^{-2} s^{-1}, which is about 3.6 times higher than that evaluated in the previous ultra-long discharge without the ML. The wall inventory continued to increase during the discharge and finally reached up to 8 x 10^{21} atoms at the end of the discharge. No Long time global balance between particle absorption and release of the wall was observed. It seems to be attributed to suppression of the hydrogen release from the wall due to less temperature increase by the insert of the ML. We have investigated the spatial structure of hydrogen recycling of the long duration discharge with the ML. The toroidal structure of hydrogen recycling changes only at the ML and its neighborhood, and the other part, i.e. main chamber recycling, still remain the same structure as that without the ML. Moreover, it is found that the structure of the main chamber recycling is the same in the low and high density cases. It suggests that the charge exchange neutral dominates the main chamber recycling. The contribution ratio of the main chamber to the wall recycling decreases by about half due to the ML. That of the section of the ML reaches about 45%. The characteristic length λ_{LIM} of the broadening of the profile of $I_{H\alpha}$ originating at the limiter is ~0.33 m for low density ($\bar{n}_e$~0.1x10^{19} m^{-3}) discharge such as the ultra-long one and ~0.22 m for high density ($\bar{n}_e$~1x10^{19} m^{-3}) discharge. It is found that λ_{LIM} does not change so much even though the density changes by the one order of magnitude. It suggests that the broadening of the profile at the limiter is attributed to the transport of the neutrals through the SOL.

Acknowledgement

The authors are grateful to Drs. S. Takamura and N. Ohno for useful discussions. This work has been partially performed under the framework of joint-use research in RIAM Kyushu university and the bi-directional collaboration organized by NIFS. This work is partially supported by a Grant-in-Aid for Science Research from Ministry of Education, Culture, Sports, Science and Technology.

References

[1] Equipe Tore Supra (presented by F. Saint-Laurent), Nucl. Fusion **40** (2000) 1047.
[2] J. Jacquinot, et al., Nucl. Fusion **43** (2003) 1583.
[3] D. van Houtte, et al., Nucl. Fusion **44** (2004) L11.
[4] M. Sakamoto, et al., Nucl. Fusion **42** (2002) 165.
[5] M. Sakamoto, et al., J. Nucl. Mater. **313-316** (2003) 519.
[6] Y. Hirooka, et al., J. Nucl. Mater. **313-316** (2003) 588.
[7] M. Sakamoto, et al., Nucl. Fusion **44** (2004) 693.
[8] P.K. Mioduszewski and L.W. Owen, J. Nucl. Mater., **290-293** (2001) 443.
[9] E.S. Marmar, J. Nucl. Mater., **76-77** (1978) 59.
[10] L. W. Owen, et al., J. Nucl. Mater., **176-177** (1990) 803.
[11] S. Morita, et al., Transactions of Fusion Tech., **27** (1995) 239.
[12] H. Kojima and S. Takamura, Jpn. J. Appl. Phys. **41** (2002) 6557.
[13] H. Zushi, et al., Proc. of 31th EPS (2004) P2.129.